EXPERIMENTAL INVESTIGATIONS ON THE MECHANICAL PROPERTIES OF NEW TYPE OF INTERPENETRATING PHASE COMPOSITE BASED ON SCHWARTZ PRIMITIVE TRIPLY PERIODIC MINIMAL SURFACES

Oraib Al-Ketan[1] and Rashid K. Abu Al-Rub[1]
[1]Masdar Institute of Science and Technology, Mechanical and Materials Engineering Department, Abu Dhabi, UAE
Email: ogalketan@masdar.ac.ae

Keywords: Triply periodic minimal surfaces (TPMS), additive manufacturing, 3D printing, scanning electron microscopy (SEM).

Abstract

A new type of interpenetrating phase composite (IPC) is introduced in this work. The composite has a reinforcement phase designed mathematically based on Schwartz Primitive (P) triply periodic minimal surfaces (TPMS). The P-TPMS based IPC was fabricated using the technique of Polyjet 3D printing. Scanning electron microscopy (SEM) was used to assess the quality of printing. Periodicity, aging, and anisotropy effects on the mechanical properties were investigated. The experimental results obtained showed that at least two unit cells are required to obtain the effective mechanical properties. The samples proved to be very sensitive to aging effect and printing direction.

1. Introduction

The importance of composite materials lies in their ability to combine the properties of their constituents. Their properties can be tailored to fit the desired application. Engineers have tried for long to emulate the multi-functionality offered by biomaterials [1-12], the lightweight human bone for instance provides the necessary strength to support the human body. Similarly, the very soft molluscans are protected by the ultra-light, yet strong, coiled-shell to which they are attached. In this work, a new mathematically-developed three-dimensional (3D) reinforcements for composites, which are found in nature, based on triply periodic minimal surfaces (TPMS) is introduced. TPMS are mathematically designed non-self-intersecting surfaces that are intertwined in 3D space and locally minimize surface area. Such surfaces can be observed in soap films formed in rigid frames and nature species [13]. These new periodic architectures have properties that are controlled by their engineered geometry (topology) rather than by atomic composition alone.

The fabrication of highly complex interconnected structures was a challenge that faced engineers for long because of the limitations in traditional manufacturing processes. Yet the need to mimic the topologies of bio-inspired materials was significant, for they offer a wide range of multi-functionality. Recent advances in fabrication methods not only facilitated the fabrication of complex structures but also insured high levels of control over the quality of these parts. Additive manufacturing, commonly known as 3D printing, has lately gained much attention for being a large umbrella covering many possible industrial applications. Recently, 3D printing has provided a successful large scale cost-effective industrialized approach in several engineering areas [14].

In this work, the well-known Schwarz Primitive (P) TPMS (Figure 1) is used as a single, continuous, smooth-curved, thin shell, hard material reinforcement phase in the IPC, where the matrix is a soft obedient rubbery material. The volume fraction of the reinforcing phase is controlled by varying its thickness. A shell

Excerpt from ISBN 978-3-00-053387-7

is defined as a curved solid surface structure that supports external loads mainly through coplanar stresses [15]; therefore, it is anticipated that when shells take the form of the P-TPMS an improved resistance to external loads is achieved.

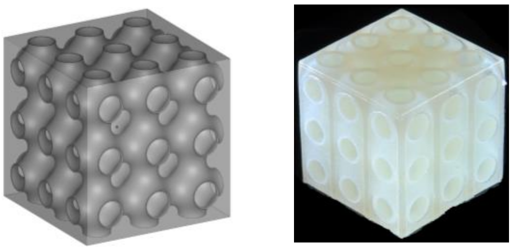

a) b)

Figure 1: a) CAD file of the P-IPC and b) fabricated P-IPC-sample.

The following sections will be arranged as follow: first the design and fabrication of the IPC is discussed in the second section. The third section presents the experimental setup. Fourth and fifth sections are dedicated for the discussion of the results and the conclusions, respectively.

2. Design and Fabrication

The mathematical-based P-IPC structure was first designed in a computer aided design (CAD) software. The CAD file was then exported as stereolothography file (STL) and sliced to layers with 16µm thickness ready to be printed using Polyjet technology 3D printing in the Connex 260 3D printer from Stratasys which permits simultaneous printing of two different materials. For that purpose, TangoPlus (a soft rubbery material) was used as the matrix and Verowhite (a rigid opaque photopolymer) was used as the reinforcement phase. Both materials were injected and were cured by UV light. The mechanical properties of these materials are presented in Table 1.

Table 1: Summary of mechanical properties of base materials in printing direction [16].

Material	Young's Modulus [MPa]	Ultimate compressive strength [MPa]	Strain at failure	Toughness [J/m$_3$]
Tango-Plus	0.3427	1.04	0.57	0.1894
Vero-white	1191	77.7	0.45	20.64

3. Experimental Setup

The linear and nonlinear mechanical properties are evaluated. First, 3 samples at least of P-IPC with single, double and 3x3x3 repeated unit cells are tested to assess the periodicity. Samples were then tested in two directions, parallel to the printing direction and perpendicular to the printing direction to assess the anisotropy introduced by 3D printing. Finally aging effect was investigated, where samples were left at room

Excerpt from ISBN 978-3-00-053387-7

conditions for 1, 17 and 60 days then tested in compression using the universal testing machine Instron with a strain rate of 0.001 /s.

4. **Results and Discussion**

First, the P-IPC with reinforcement volume fraction of 5% was tested with two periodicities, where the unit cell with a size of $L = 10$ mm, is repeated periodically on the three Cartesian directions, producing 8 and 27 unit cells for the 2x2x2 and 3x3x3 cases, respectively.

According to testing results (see Figure 2) the behavior is altered significantly when periodicity is invoked. In fact, the P_IPC with single unit cell(1x1x1) was investigated by [16] with no emphasis on the periodicity and its impact on the effective properties. The 1x1x1 (1 unit cell) Young's modulus is lower by 52% and 51.5% than 2x2x2 (8 unit cells) and 3x3x3 (27 unit cells) cases respectively. In addition, the Young's modulus of 2x2x2 and 3x3x3 cases are different only by 2%, which indicates that both periodicities exhibits comparable elastic region. Whereas for inelastic properties, 1x1x1 case produced 63% higher ultimate compressive strength in comparison to 2x2x2 and 3x3x3 cases. This implies that the interface region where unit cells link, which was invoked by periodicity are susceptible to cracking and might be the reason for the reduction in strength. The 2x2x2 and 3x3x3 exhibited almost comparable ultimate compressive strengths (15% difference). Identifying the point of failure was challenging in all the three cases (1x1x1, 2x2x2, and 3x3x3). The structure demonstrated a significant reduction in strength around a strain of 0.55, where the structure lost its geometrical integrity and densification started. The ability of absorbing energy (toughness) appears to be less sensitive to periodicity, reporting a maximum of 12 % difference.

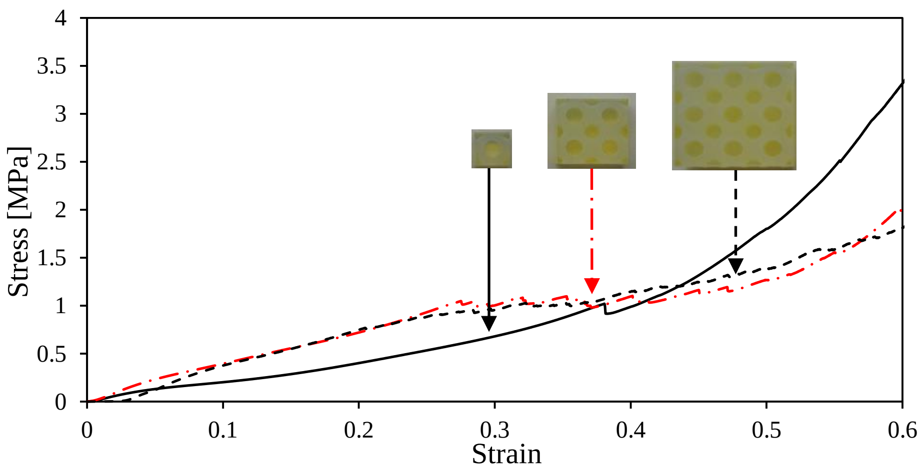

Figure 2 P-IPC with periodicity of 1 unit cell ,8 unit cells(2x2x2) and 27 unit cells (3x3x3) and their mechanical properties.

Aging effect on the mechanical properties of the P-IPC was investigated. Samples with 10% reinforcement volume fraction were kept at room conditions for 1day, 17days and 60days. The stress-strain curves for the different aged samples are plotted in Figure 3. An obvious drop in elastic properties can be observed; elastic modulus decreased by 21% after 17 days as compared to 1 day and further decreased by 42% after 60 days

Excerpt from ISBN 978-3-00-053387-7

as compared to 1 day. The yield stress also decreases by 40% and 46% for 17 days and 60 days, respectively, as compared to the 1 day. The maximum strength reduced dramatically (by 36%) after 17 days and no further reduction is observed in the samples aged for 60 days. Overall a noticeable reduction in the mechanical properties is observed with age.

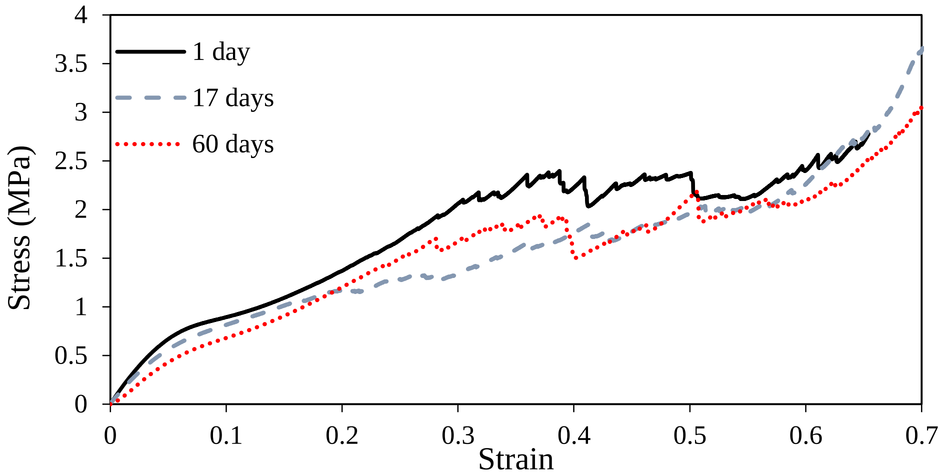

Figure 3: Aging effect on the mechanical response of the P-IPC.

After checking the periodicity and aging effects, 3x3x3 samples with 10% reinforcement volume fraction were tested in two directions; parallel and perpendicular to the printing direction to assess the anisotropy introduced by 3D printing. The anisotropy introduced due to printing is significant as can be seen in Figure 4, where a large drop in the mechanical properties is observed when testing in a direction perpendicular to the printing direction. It should be noted here that in Polyjet 3D printing, each layer is added on the previous one along a certain axis, leading to an oriented configuration for voids in the microstructure. This phenomenon can be clearly seen in the SEM images taken for the reinforcing phase separately (see Figure 5). The images show clear microscale separation between layers in the printing direction. This orientation configuration results in the anisotropic behavior of printed samples. Another factor that contributes to the anisotropic behavior is the arrangement of UV bulb in the printers as they are set such that the top of created layers parallel to UV bulbs absorbs more light energy than the side (or the thickness) surface. Therefore, the top printed layer hardens (cures) much more and leads to this anisotropic behavior[17].

Excerpt from ISBN 978-3-00-053387-7

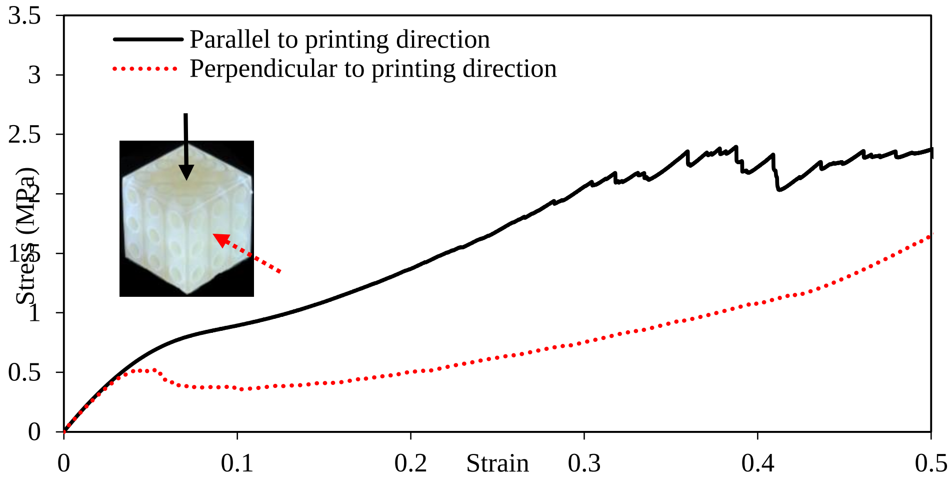

Figure 4: P-IPC tested in two directions; parallel to the printing direction and perpendicular to the printing direction.

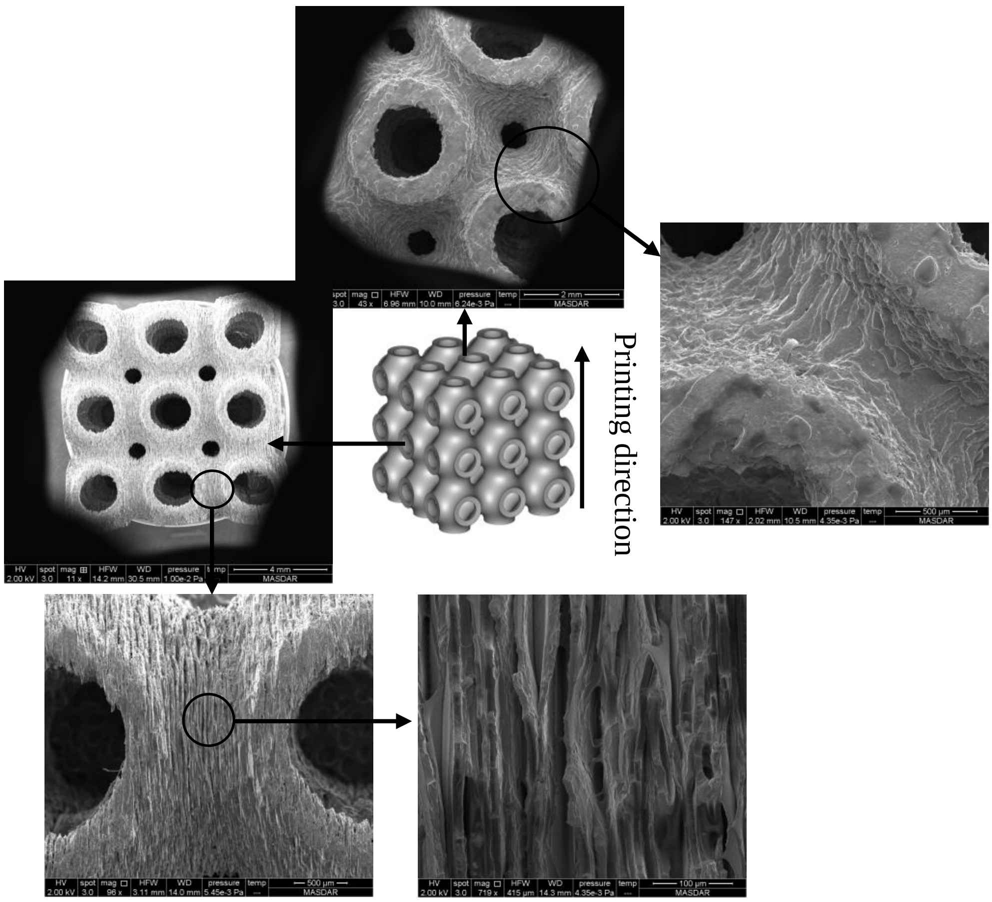

Figure 5: SEM images showing the directionality effect of the 3D printing.

Excerpt from ISBN 978-3-00-053387-7

After assessing the quality of printing, periodicity, aging, and anisotropy effects on the mechanical properties, samples were printed with different reinforcing volume fractions; 5%, 10% and 15%. The samples were fabricated and kept at room conditions for 7 days. They were then tested under compression and the results are presented in Figure 1. The results show improved mechanical properties with increasing the volume fraction of the reinforcing phase. The Young's modulus of the IPC with 5% reinforcing phase is 10 times larger than that of the Tango-plus matrix material with no reinforcement. At this volume fraction, linear elastic trend can be seen followed by a plateau stress. In fact, at the plateau stress, localized fractures are observed and can be noted in the stress-strain curve in the form of noise. At volume fraction of ≈ 10%, the stress-strain curve shows a more distinct linear elastic trend until a yield stress value is reached, after which a post yield hardening starts to take place until the stress level reaches its maximum. After the maximum strength is reached, cracks start to take place. A deterioration in the mechanical properties is observed after the maximum strength is reached and is related to the loss of stiffness associated with localized fracture events. The last stage in the curve is the densification of the two phases due to high levels of deformation. At volume fractions of 15%, the shape of the stress-stain curve remains similar; however, the Young's modulus, maximum strength and toughness increase. The mechanical properties at the three different reinforcing volume fractions are presented in Table 2.

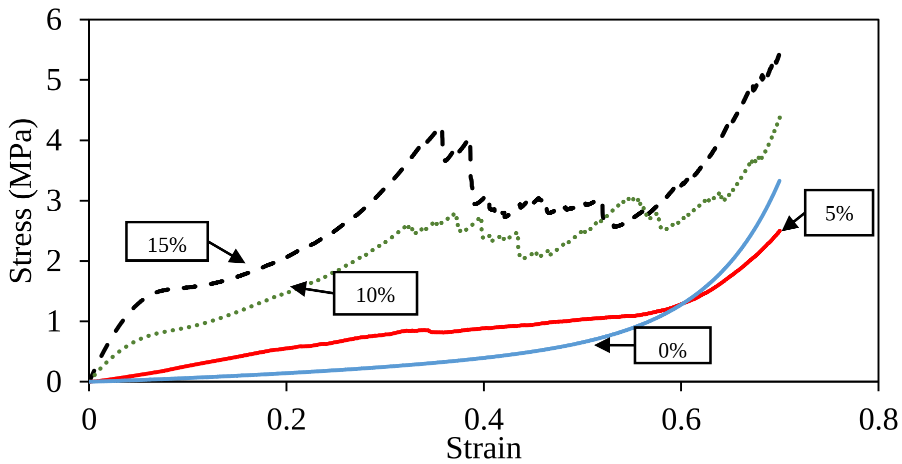

Figure 6: Typical stress strain curve for the IPC with different reinforcing volume fractions.

Table 2: Mechanical properties of the P-IPC for the 3 different volume fractions of the reinforcing phase.

Volume fraction	Young's modulus (MPa)	Toughness (j/m^3)	Maximum strength (MPa)	Yield stress (MPa)
10%	17.2	1.077	2.82	0.71
15%	28.0	1.439	4.36	1.38
24%	72.7	2.180	4.83	3.47

The P-IPC was compared with the traditional particle reinforced composite, using the same matrix and reinforcement materials and aging time. The particle reinforced composites consisted of a single unit cell with cubic lattice structure repeated 3x3x3 and the volume fraction was controlled by varying the radius of

Excerpt from ISBN 978-3-00-053387-7

the particle. The stress strain curves of the particle reinforced composites are shown in Figure 7. It is very clear that the P- IPC outperforms the traditional particle reinforced composite. The continuous nature of the IPC throughout the matrix body triggers the strain sharing mechanism between the two phases, meaning that (unlike the particle reinforced composite) both phases undergo the same strain levels at the same time, which maximizes the use of the reinforcing phase to carry and transfer the load.

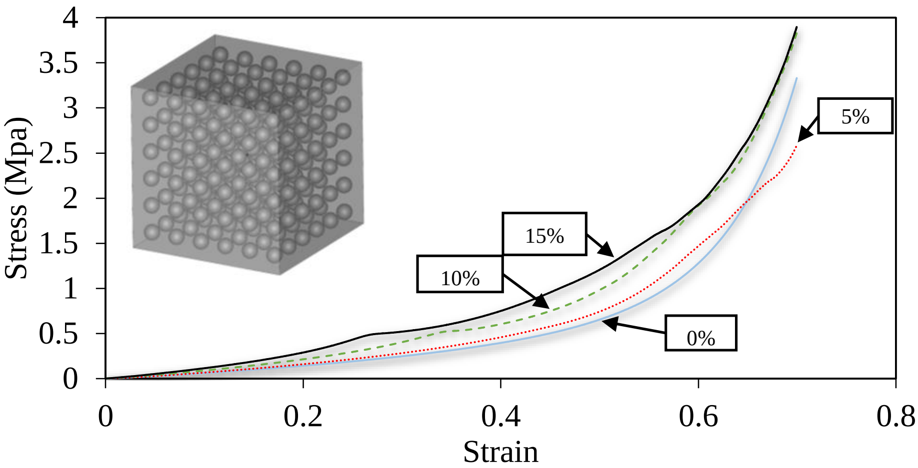

Figure 7: Typical stress strain curves for particle reinforced composite with different reinforcement volume fractions.

5. Conclusions

In summary, we have introduced and mechanically investigated a new and novel type of advanced interpenetrating phase composite where the matrix is reinforced with a single, continuous, smooth-curved, thin shell, hard material possessing the topology of Schwarz Primitive TPMS. The experimental results obtained showed that at least two unit cells are required to obtain the effective mechanical properties. However, the samples proved to be very sensitive to aging effect, where a big reduction in the overall mechanical properties was observed with time. The polyjet technology additive manufacturing that was used to print the samples introduced a directionality effect such that it was concluded that testing in the direction parallel to printing direction give better mechanical properties compared to the transverse direction due to the de-bonding of the printed layers and formation of cracks. The new IPC outperformed the traditional particle reinforced composites.

6. References

1. Abueidda, D.W., et al., *Electrical conductivity of 3D periodic architectured interpenetrating phase composites with carbon nanostructured-epoxy reinforcements.* Composites Science and Technology, 2015. **118**: p. 127-134.
2. Abueidda, D.W., et al., *Micromechanical finite element predictions of a reduced coefficient of thermal expansion for 3D periodic architectured interpenetrating phase composites.* Composite Structures, 2015. **133**: p. 85-97.

3. Abueidda, D.W., et al., *Finite element predictions of effective multifunctional properties of interpenetrating phase composites with novel triply periodic solid shell architectured reinforcements.* International Journal of Mechanical Sciences, 2015. **92**: p. 80-89.
4. Abu Al-Rub, R.K., D.W. Abueidda, and A.S. Dalaq, *Thermo-electro-mechanical properties of interpenetrating phase composites with periodic architectured reinforcements*, in *From Creep Damage Mechanics to Homogenization Methods*. 2015, Springer International Publishing. p. 1-18.
5. Chernow, V., et al., *Polymer lattices as mechanically tunable 3-dimensional photonic crystals operating in the infrared.* Applied Physics Letters, 2015. **107**(10): p. 101905.
6. Compton, B.G. and J.A. Lewis, *3D-Printing of Lightweight Cellular Composites.* Advanced Materials, 2014. **26**(34): p. 5930-5935.
7. Lee, J.H., J.P. Singer, and E.L. Thomas, *Micro-/Nanostructured Mechanical Metamaterials.* Advanced materials, 2012. **24**(36): p. 4782-4810.
8. Lee, S.-W., et al., *Size Effect Suppresses Brittle Failure in Hollow Cu60Zr40 Metallic Glass Nanolattices Deformed at Cryogenic Temperatures.* Nano letters, 2015. **15**(9): p. 5673-5681.
9. Meza, L.R., et al., *Resilient 3D hierarchical architected metamaterials.* Proceedings of the National Academy of Sciences, 2015. **112**(37): p. 11502-11507.
10. Montemayor, L., V. Chernow, and J.R. Greer, *Materials by design: Using architecture in material design to reach new property spaces.* MRS Bulletin, 2015. **40**(12): p. 1122-1129.
11. Wang, L., et al., *Co-Continuous composite materials for stiffness, strength, and energy dissipation.* Advanced Materials, 2011. **23**(13): p. 1524-1529.
12. Xia, X., X.W. Gu, and J.R. Greer, *3D Architected Si-Cu Core-Shell Nanolattices As Mechanically Robust, Binder-Free Li-Ion Battery Electrodes.* Meeting Abstracts, 2015(47): p. 1915-1915.
13. Hyde, S., et al., *The language of shape: the role of curvature in condensed matter: physics, chemistry and biology*. 1996: Elsevier.
14. Wohlers, T., *3D Printing and Additive Manufacturing State of the Industry.* Annual Worldwide Progress Report, 2015.
15. Han, S.C., J.W. Lee, and K. Kang, *A New Type of Low Density Material: Shellular.* Advanced Materials, 2015. **27**(37): p. 5506-5511.
16. Dalaq, A.S., D.W. Abueidda, and R.K.A. Al-Rub, *Mechanical properties of 3D printed interpenetrating phase composites with novel architectured 3D solid-sheet reinforcements.* Composites Part A: Applied Science and Manufacturing, 2016. **84**: p. 266-280.
17. Kadkhodapour, J., H. Montazerian, and S. Raeisi, *Investigating internal architecture effect in plastic deformation and failure for TPMS-based scaffolds using simulation methods and experimental procedure.* Materials Science and Engineering: C, 2014. **43**: p. 587-597.

Excerpt from ISBN 978-3-00-053387-7